

# **Investigation of Forged-Like Microstructure Produced by A Hybrid Manufacturing Process**

Romy Francis\*, Joseph W Newkirk<sup>†</sup>, Frank Liou\*

\*Mechanical Engineering,

<sup>†</sup>Materials Science and Engineering

Missouri University of Science and Technology, Rolla MO 65409

REVIEWED

## **Abstract**

Laser Metal Deposition (LMD) is an additive manufacturing technique for manufacturing complex near net shaped components. The grain size of the typical deposition microstructure in case of Ti-6Al-4V can range between 100 $\mu$ m-600 $\mu$ m, which is much larger than that of forged-like microstructures. Friction Stir Processing (FSP) has been investigated as a method for surface modification to form refined microstructure at the surface of the Ti-6Al-4V components manufactured from the LMD method. Integration of FSP and LMD can greatly improve the product properties. Friction stir processing of the laser deposited Ti-6Al-4V deposits was performed and optimum processing parameters were obtained using this hybrid process. The microstructure of the nugget regions obtained in the substrate weld, stir over deposit and deposit over stir experiments is presented. A much decreasing grain size was observed in the dilution zone inside the nugget from the stir surface to the bottom of the dilution zone.

## **Introduction**

Laser Metal Deposition (LMD) is an additive manufacturing technique which is used for fabricating complex near net shaped components. This technology utilizes fewer raw materials and takes less time in producing the final component. The part obtained after the deposition requires minimal machining and this is an added advantage of this process over the conventional manufacturing processes. The microstructure obtained through this process is dependent on the laser deposition parameters which include the laser power, laser scanning speed, the powder feed rate etc [1]. Typical deposition microstructure in case of Ti-6Al-4V consists of a basketweave Widmanstätten  $\alpha$  morphology and colony Widmanstätten  $\alpha$  morphology inside a prior  $\beta$  grain, continuous  $\alpha$  along prior  $\beta$  grains have also been observed [2]. The grains can range between 100 $\mu$ m-600 $\mu$ m. The lamellar structure results in better creep properties and higher fracture toughness [3] whereas the equiaxed structures resist fatigue crack initiation.

Friction Stir Processing (FSP) has been investigated as a method for surface modification to form refined microstructure at the surface of the Ti-6Al-4V components manufactured from this method. In the past, FSP has been used to improve mechanical properties like the low cycle fatigue properties, hardness, corrosion resistance, and resistance to crack initiation in Al, Ni, Fe, Cu and Ti alloys [4, 5, and 6]. FSP works on the principles of Friction Stir Welding (FSW) [7] patented by TWI, UK. The only difference being that in case of FSP no weld is formed. The rotating non consumable tool consisting of a pin made from a refractory metal plunges into the material to be processed till the tool shoulder makes contact with the work piece. Once the tool shoulder makes contact, the tool is traversed in X or Y direction based on the clamping constraints of the work piece. The material under the shoulder is plastically deformed and is

thermo-mechanically processed due to the compressive forces and the churning action induced by the rotation of the tool. This deformation is accompanied with high strain rates and the process yields highly refined microstructure. Research was conducted earlier in LAMP lab to evaluate methods to form work hardened and re-crystallized layer of the LMD Ti-6Al-4V parts [2]. Depths of up to 1000 $\mu$ m were obtained by rotational burnishing and up to 10  $\mu$ m were obtained by aggressive milling. Integration of FSP in LAMP lab is a step further in this direction to improve the product properties. Cooling rate in case of laser deposits is very high and hence FSP can also be used to eliminate the internal stress if any. Lack of fusion voids [8] caused at the substrate-deposit interface can also be addressed by FSP.

Metal forging is a metal forming process that involves applying compressive forces to a work piece to deform it, and create a desired geometric change to the material. Metal forging is known to produce some of the strongest manufactured parts compared to other metal manufacturing processes. This paper summarizes a hybrid manufacturing process, including an LMD and a FSP, for producing or repairing parts with forged-like microstructure.

## **Experimental Methodology**

### **Equipment and Deposition Process Overview**

Friction stir processing (FSP) was performed using FADAL 3016 CNC which is part of the multi axis hybrid laser deposition system at the Missouri S&T LAMP lab. The 1kW Nuvyonx diode laser (808 nm) forms the second part of the hybrid laser deposition system. The laser system comprising of the laser cladding head, focusing optics, powder delivering hoses is attached to the Z axis of the CNC. Atomized metal powder is delivered from a powder feeder to the laser melt pool on the substrate while the X-Y axes of the CNC moves as per the G and M codes fed to it via the control system to deposit the 2D cross-section of the part. When one macro layer is deposited, the Z axis moves up by a predetermined height to refocus the laser to form melt pool on the previously deposited layer and follow the build pattern for deposition. The approximate bead width in case of deposition with Ti-6Al-4V is 3mm. The deposition was carried out at 780 watts laser power with melt pool size of 2mm and table speed of 5 mm/s. A 15 % overlap of the tracks was maintained while deposition. Three laser deposits approximately 47mm x 26mm x 10mm in dimension were then deposited on a 50mm x 108mm x 9.5mm Ti 6Al-4V substrate. The deposition parameters of these deposits were not expected to significantly affect FSP. Ti-6Al-4V powder was supplied by Accumet Materials Co and was to the order of -100 +325 mesh.

### **Friction Stir Processing**

Two different stepped FSP tools manufactured from Densimet-176 were used for this study. The tool shoulder did not have any features and no lead angle was used during the run. Each tool consisted of a stepped pin profile resembling an inverted wedding cake. Each step acted as a shoulder, helped in heat buildup and plastic deformation resulting in better processing. The step diameters were 2.8mm, 3.5mm, 4.5mm and tool shoulder diameter was 7.6 mm. The steps were 0.5mm deep in case of Tool-1 and 1mm in case of Tool-2 (Figure 1).



Figure 1. Stepped pin profile Tool-2

Atmospherically sealed argon gas enclosure was used to prevent oxidation of the tool and Ti 6Al-4V deposit during FSP. Multiple trials were previously conducted with both the tools to obtain defect free stir surfaces before this run was performed. Tool traverse feed of 50.8 mm/min (2 IPM) yielded better stir surface finish and it also maintained the tool integrity. It was observed that the Tool-1 required approximately 10% higher RPM than Tool-2 which was being operated at 275 RPM to attain the intended plunge. This was due to the fact that only limited heat buildup was obtained with a shorter pin profile at the same parameters. This meant that even though Ti-6Al-4V had a low thermal conductivity it was high enough to dissipate the thermal energy into the surrounding material requiring higher RPM for attaining plunge and subsequent plastic deformation. The processing parameters used for the experiment has been summarized in Table 1.

Table 1 Friction stir processing parameters

Run ID	Plunge Feed	Traverse Feed	RPM
T1-103007.1 †	1.27 mm/min	50.8 mm/min	300
T2-102907.1	1.27 mm/min	50.8 mm/min	275
T1-103007.2	1.27 mm/min	50.8 mm/min	300
T2-102907.2	1.27 mm/min	50.8 mm/min	275
T1-103007.3	1.27 mm/min	50.8 mm/min	300
T2-102907.3	1.27 mm/min	50.8 mm/min	275

† All the stir runs have been named in the following manner (Type of tool) - (Month) (Date) (Year). (Run serial No: for that day)

Three sets of experiments were performed with each tool to evaluate the effects of FSP on the laser deposits. The first set comprised of laying one track of stir each with both the tools side by side on the same laser deposit. Second set of experiment was performed to study the effect of laser interaction with the stir zone (SZ). Single, double and triple pass of single track laser deposition was performed on top of the stir region in addition to FSP of laser deposit. Third set of experiment consisted of stirring through the deposit into the substrate. This sample was obtained by milling off the existing laser deposit to leave approximately 1 mm of deposit on the substrate.

### Sample Preparation

The stirred samples were cross-sectioned perpendicular to the stir direction using resin bonded silicon carbide rotary blades. Samples were mounted using Diallyl Phthalate epoxy resin. Grinding and polishing was performed on a LECO Spectrum System 1000 automatic polisher. Blue, green and red cameo platinum plates corresponding to 120~180, 220~280 and 600 grit

were used for initial grinding. Two step polishing was performed using 9 micron diamond solution and 0.05 micron colloidal silica on imperial cloth. The samples were rinsed thoroughly in water after the first polishing medium. It was then placed in an ultrasonic bath of 95% ethyl alcohol for 20 minutes to clean off the final polishing medium.

**Analysis**

Vickers microhardness test was performed using the Struers Duramin 5 hardness testing machine with a load of 9.81N for 10 seconds. Three columns of 16 microhardness indents each were made on the samples. Three indent columns represented the advancing side of the nugget (N/4), centerline of the nugget (N/2) and the retreating side of the nugget (3N/4). The indents were separated by 250 micros to ensure that the readings were not biased. The samples were then etched with modified Kroll’s reagent (5ml HF, 22.5ml HNO<sub>3</sub>, 22.5ml HCl) for approximately 15 seconds. The microstructure was later characterized using the Hitachi S570 scanning electron microscope, Hitachi S4700 Field emission microscope and the Nikon Epiphot 300 optical microscope. Backscattered compo mode was used for imaging in SEM.

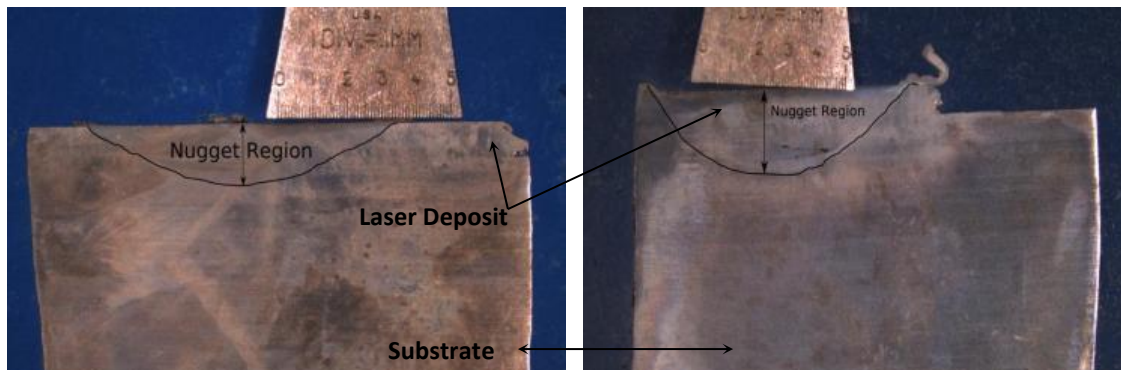
**Results and Discussion**

**Microstructural Evolution**

**Substrate Welding Experiment-Stir Zone:** The nugget cross-section (c/s) was shallower in case of T1-103007.3 compared to T2-102907.3 (Figure 2 a, b) since a shorter tool was used. In both the cases the nugget c/s was observed to be nearly parabolic. The overall nugget cross-section consisting of the SZ, TMAZ (Thermomechanically Affected Zone) and HAZ (Heat Affected Zone) was outlined with an image editing software after etching the samples with modified Kroll’s reagent. The observed depth at the center of the nugget (N/2) has been summarized in Table 2. In both cases, the FSP nugget region extended into the substrate through the laser deposit as per the requirements of the experiment.

Table 2 Substrate weld nugget depths

Run No:	Avg FSP Nugget depth (µm)
T1-103007.3	1670±25
T2-102907.3	2500±20



(a) Run No: T1-103007.3 Substrate Welding (b) Run No: T2-102907.3 Substrate Welding  
Figure 2. Substrate welding experiment

The temperature profile obtained from the optical pyrometer aimed at the tool shank slightly above the shoulder indicated that the tool shank temperature did not exceed 815°C which strongly indicates that the processing conditions existing underneath the tool shoulder would have been below Beta transus (995-1010 °C). The equiaxed microstructure of the substrate approx 16µm (Figure.3) and the Widmanstätten, lamellar morphology with  $\alpha+\beta$  laths in the prior  $\beta$  grains (Figure 4) of the deposit region was transformed into highly refined, re-crystallized primary  $\alpha$  microstructure (Figure 5) which had a diameter of around  $0.805 \pm 0.080 \mu\text{m}$ . The grain size was measured by linear intercept method as per ASTM 112[9].

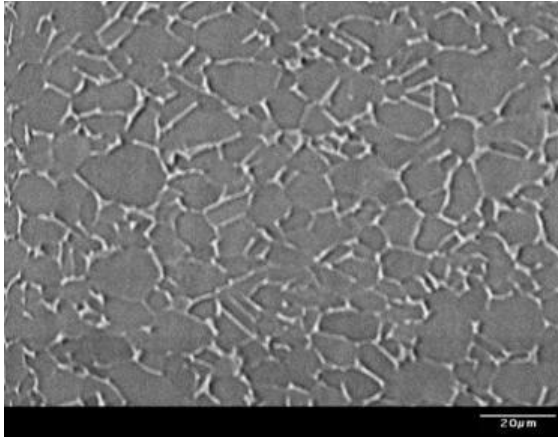


Figure 3. Equiaxed substrate microstructure

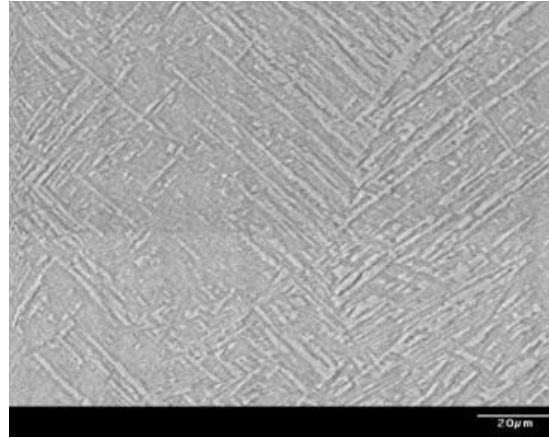


Figure 4. Basketweave structure

Rubal et.al [3] observed similar morphology in the SZ when sub transus FSP was performed on near alpha Ti-5111 alloy. FSP studies on investment cast Ti-6Al-4V conducted by Pilchak et al [5, 10] also showed equiaxed primary  $\alpha$  microstructure in the sub transus FSP SZ. The microstructure was homogenized throughout the SZ converting the parent microstructures to primary  $\alpha$ .

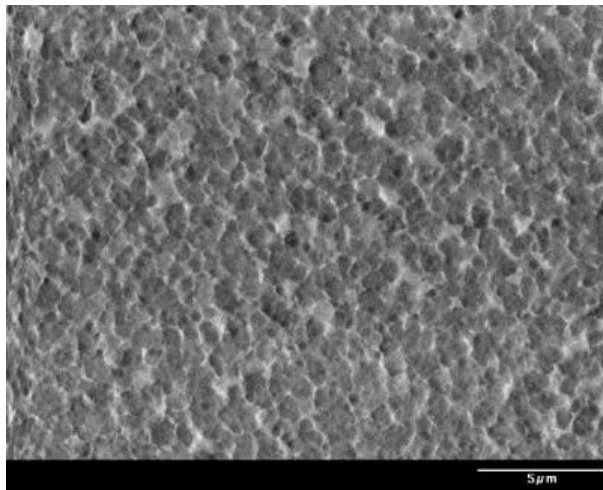


Figure 5. Equiaxed primary  $\alpha$  grains

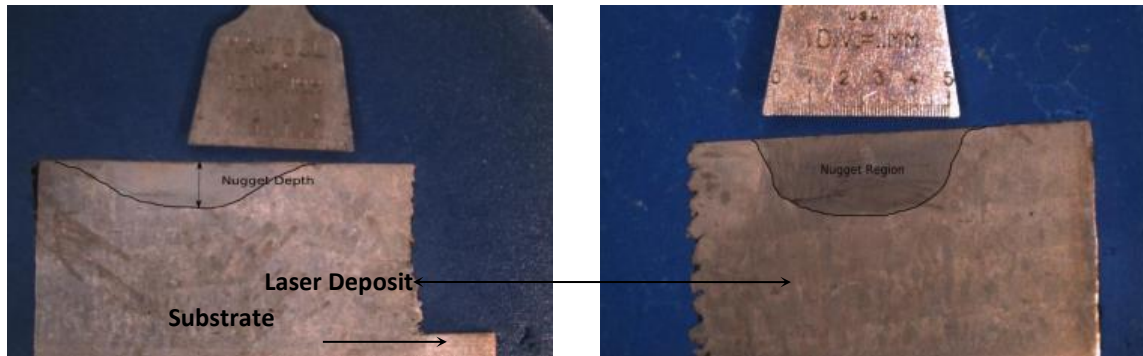
Ramirez et al [4] observed that the SZ microstructure was dependent on the processing conditions namely tool traverse feed, tool RPM, forge force, tool design, shoulder features etc

and not on the starting base material. The SZ microstructure observation is in agreement with that finding. Although stir no: T1-103007.3 was performed at a higher RPM of 300, the SZ microstructure observed was similar to the T2-102907.3 indicating that the processing conditions during that run were also sub transus. Pilchak et al [11] reported that the if the material is being worked upon by the tool during its cooling from the  $\beta$  transus then the dislocation density in the subsequently formed primary  $\alpha$  would be high. In this case, although the stir zone did not experience  $\beta$  transus there is a possibility of high dislocation density being present from the decomposition of  $\alpha+\beta$  phase.

**Stir over laser deposit-Stir zone:** The etched nugget (c/s) for both T1-103007.1, T2-102907.1 (Figure 6. a, b) was not nearly as parabolic as observed for the substrate weld experiment. The reason for this could be that the difference in the BM caused different thermal cycles and heat dissipation patterns. The bottom of the nugget region was observed to be much more flat. The SZ in case of this particular experiment also showed highly refined grains to the order of 1 micron. The depth at the center of the nugget region has been summarized in Table 3.

Table 3 Stir over deposit nugget depths	
Run No:	Avg FSP Nugget depth ( $\mu\text{m}$ )
T1-103007.1	1578 $\pm$ 23
T2-102907.1	2287 $\pm$ 19

Although the tool processed the regions totally inside the laser deposit, the resulting microstructure consisted of equiaxed primary alpha grains. As discussed earlier, the microstructure of the laser deposit is primarily lamellar. **SZ microstructure observation is in agreement with Peters et al [12] who reported that the diameter of the recrystallized  $\alpha$  grains in the thermomechanically processed bulk Ti-6Al-4V generally correspond to the width of the  $\alpha$  lamellae in the BM.** In this case the BM being the laser deposit, the  $\alpha$  lamellae is to the order of  $\sim$ 1-2 $\mu\text{m}$ . The temperature history showed that the tool shanks did not experience temperatures more than 820  $^{\circ}\text{C}$ .



(a) Stir Over Deposit Run No: T1-103007.1

(b) Run No: T2-102907.1

Figure 6. Mounted cross sections-stir over deposit

**Transition Zone (TZ) / Thermomechanically Affected Zone (TMAZ):** Zhang et al [13] reported a sharp boundary (SB) with no TMAZ in FSW of Ti-6Al-4V plates. It was reported that the deformation characteristics of TMAZ may have been masked by the subsequent phase transformations. Ramirez et al [4] observed an extremely narrow TMAZ (~10 $\mu$ m) zone. However extensive presence of equiaxed  $\alpha$  was observed in this region. TZ which is analogous to this region was proposed by Pilchak et al [11] as the region between the HAZ and the SZ which experiences measurable strain, but where the strain induced temperature gradient was insufficient to cause recrystallization as in SZ. However, gradual change from the BM to SZ microstructure was observed in the substrate weld experiment. Microstructure of the BM being a beta annealed structure. **The zone observed was approximately 70-80 $\mu$ m wide (Figure 7). This could be explained due to the fact that stirring deformation imparted from the SZ was primarily being resisted by the  $\beta$  annealed microstructure of the substrate. SZ microstructure, which was being formed as a result of dynamic recrystallization (DRX) from two different starting microstructures would have caused thermal conductivity gradient between the SZ and BM leading to a wider TZ.** The TZ microstructure was observed to consist of deformed  $\alpha/\beta$  lamellae and also equiaxed primary  $\alpha$  (Figure 8). These grains were of the order of 1 $\mu$ m.

Ramirez, Pilchak et al[4, 11] observed similar morphologies in the TZ/TMAZ which was explained by lamellar  $\alpha$  recrystallization which in case of  $\alpha+\beta$  is called  $\alpha$  globularization [14]. Seshacharyulu[14] *et al.* developed a microstructural deformation mechanism map for Ti 6Al-4V and based on that the existing strain rates in this region should be between 10<sup>-3</sup> s<sup>-1</sup> to 10<sup>-2</sup> s<sup>-1</sup> since the temperature at the SZ boundary is expected to be between 820° c and  $\beta$  transus.

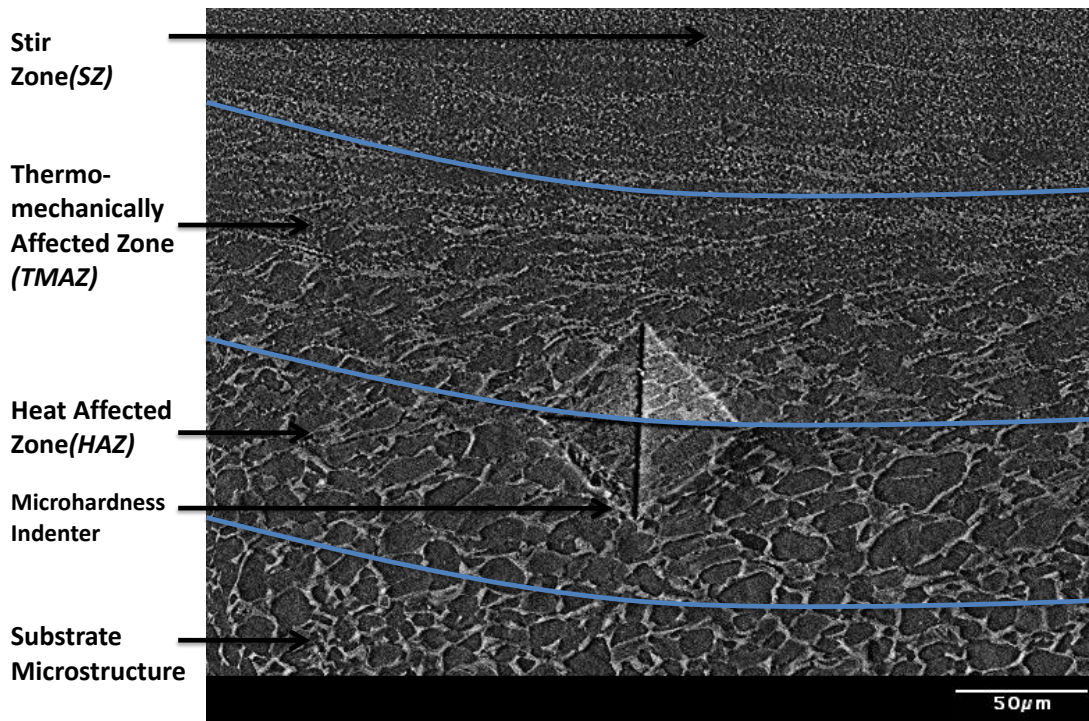


Figure 7. Nugget Morphologies- T2-102907.3

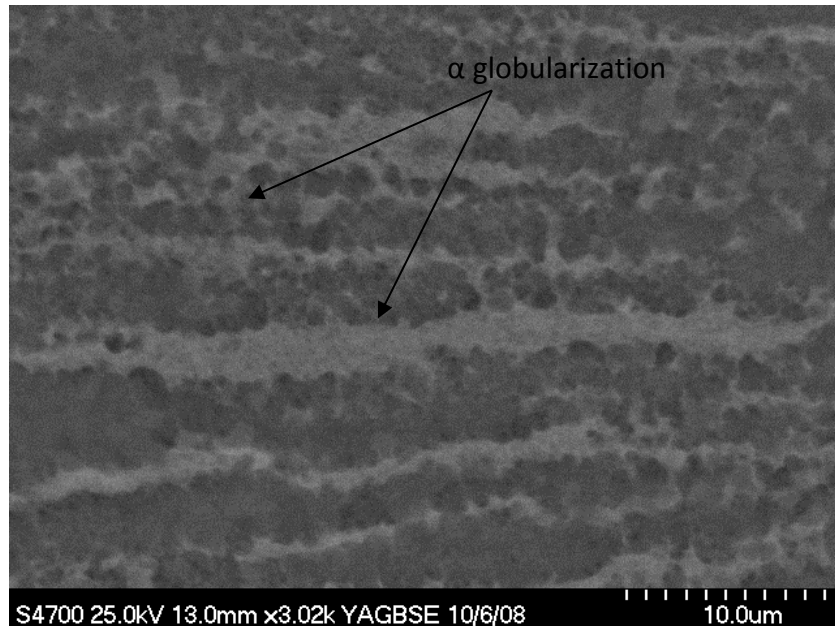


Figure 8. Equiaxed  $\alpha$  structure along with deformed lamellae in TMAZ

**TZ/TMAZ-Stir over laser deposit:** TZ observed in this case was vastly different from the one which was observed in the substrate weld experiment. The TZ existed (Figure 9) but was only of the order of 25-30 $\mu$  as compared to almost 70 $\mu$ m which existed in the substrate weld. **The shearing mechanism from the adjacent SZ could be related to this observation of abrupt change in the microstructure.** Observations made in TZ of the FSP laser deposit is in agreement with Pilchak et al [11] who reported that the morphology of TZ is a function of lamellar  $\alpha$  orientation of the adjacent BM, depth from surface and its location (AS/RS). Moreover it is clear with observations from TZ in both the substrate weld experiments that the TZ microstructure is more dependent on the BM microstructure.





Figure 9. Narrow TZ on AS of the FSP Laser Deposit

**Microstructural evolution in the deposit over stir experiments:** Regions with varying microstructures were observed when cross-sections from the laser deposition over the stir zone were studied. These regions included the deposit, dilution zone (DZ),  *$\beta$  transus zone ( $\beta$ Z)*, stir zone (SZ) and transition zone (TZ). The SZ and TZ morphology did not differ from the previously described microstructures for the FSP over laser deposits.

The heat source from the laser would be primarily utilized in (a) *melting the powder which is being deposited* and (b) *re-melting the already deposited layer* (in this case it would be the FSP layer). It is clear from Figure 10 that the first layer of the deposit over the SZ *consisted of large equiaxed grains* which to the order of 200 $\mu$ m. The dilution zone in the FSP nugget showed a grain size gradient. Decreasing equiaxed grain size was observed as the depth increased from the surface of the stir. This observation can be explained as the additional heat energy supplied by the laser aided the growth of the earlier refined equiaxed primary  $\alpha$  grains which was formed from FSP. More heat was absorbed by the grains closer to surface and the remaining heat aided in the grain growth of the primary  $\alpha$  in the dilution zone.

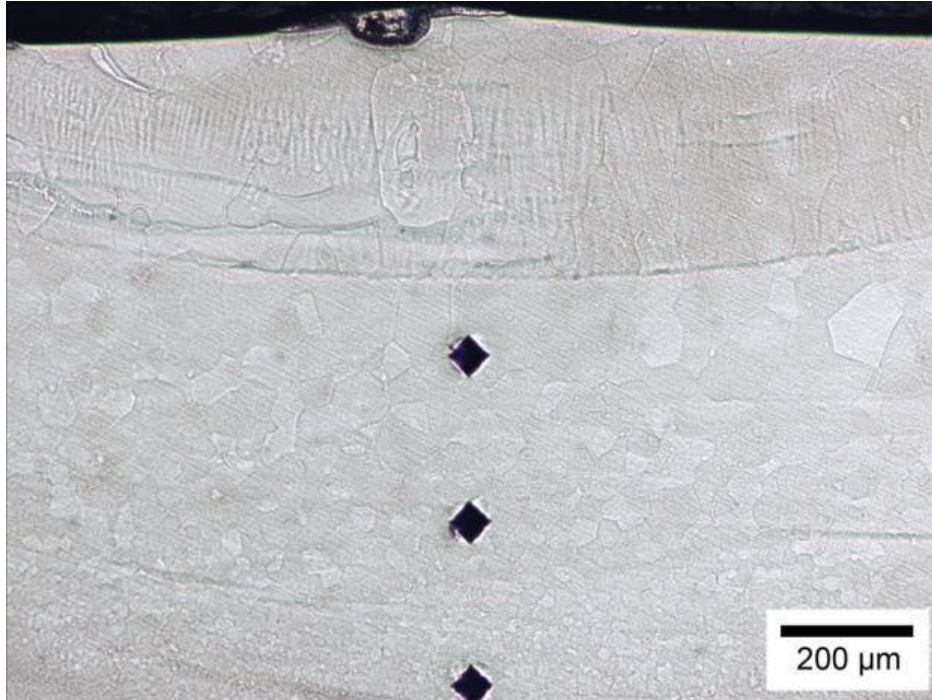


Figure 10. Center of the single track-single pass deposition over run no: T1-103007.2

Backscattered SEM imaging of an area very close to the deposit in run T2-102907.2 with triple pass of laser revealed the grain morphology as shown in Figure 11. The morphology clearly shows a fine basketweave microstructure inside a prior  $\beta$ . It is evident that this region experienced temperatures above the  $\beta$  transus.

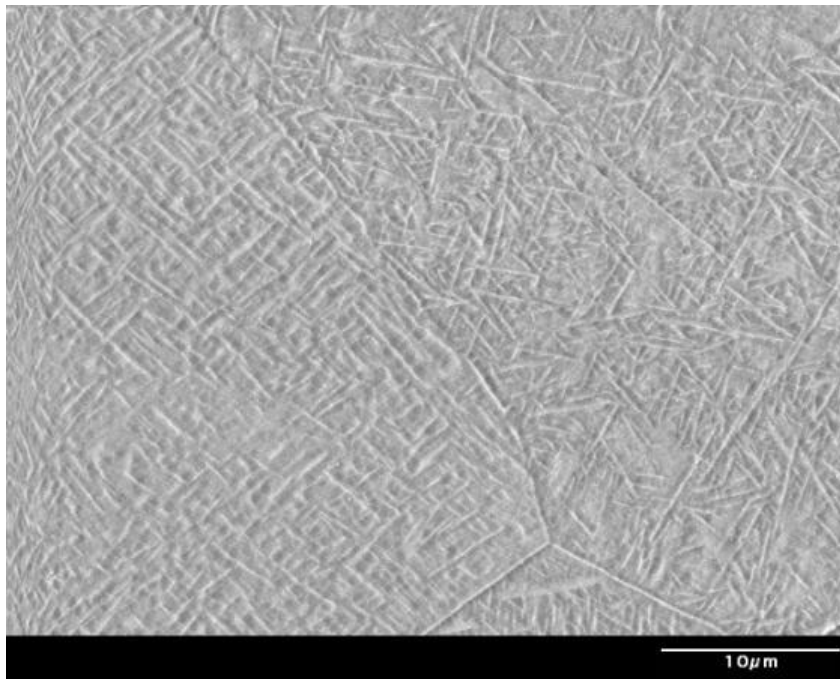


Figure 11. Fine basket weave structure close to the deposit over the stir region

It was also observed that in all the deposition over the SZ (single, double and triple pass) a clear region of approximately 100 $\mu$ m wide existed around the dilution zone. This interface consisted of extremely fine grains and it was evident that these grains did not experience temperatures above  $\beta$  transus. The same has been shown in the following Figures 12 a and b.

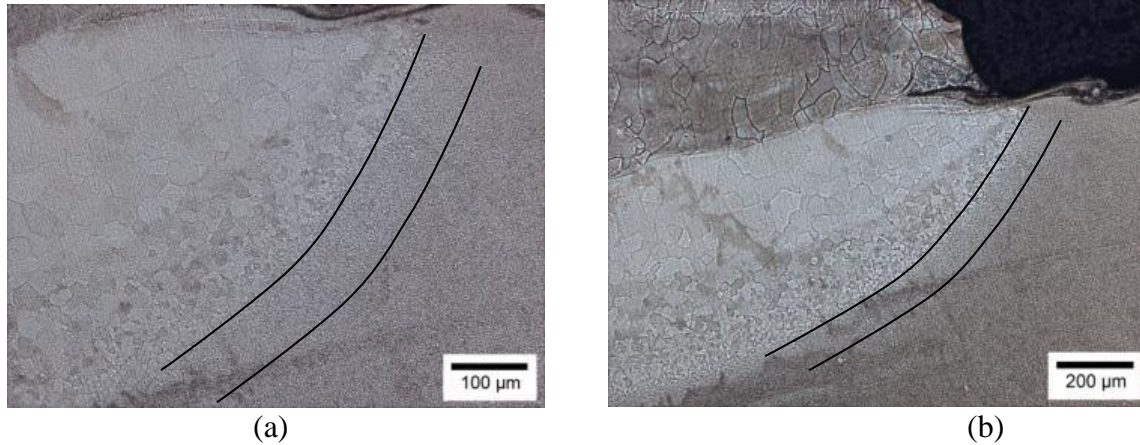


Figure 12. (a) Untransformed Zone (Higher magnification), (b) Untransformed Zone (Lower magnification)

### Microhardness

**Substrate weld microhardness:** Microhardness test data of the nugget center (N/2) of runs: T1-103007.3 and T2-102907.3 revealed that the hardness had increased noticeably in both the runs in the nugget region. Tool-2 which was processed at a lower RPM imparted more hardness to the SZ compared to Tool-1. This could have been observed due to the fact that lower processing temperatures which existed due to a lower RPM may have added more dislocations during the processing. Similar trends were observed when the microhardness data was compared on the advancing side (N/4) and the retreating side (3N/4). It is worthwhile to note that the hardness kept decreasing as a function of depth which can be explained as more plastic strain was imparted by the tool shoulder at the top of the nugget compared to the remaining volume inducing more hardness near the top of the nugget.

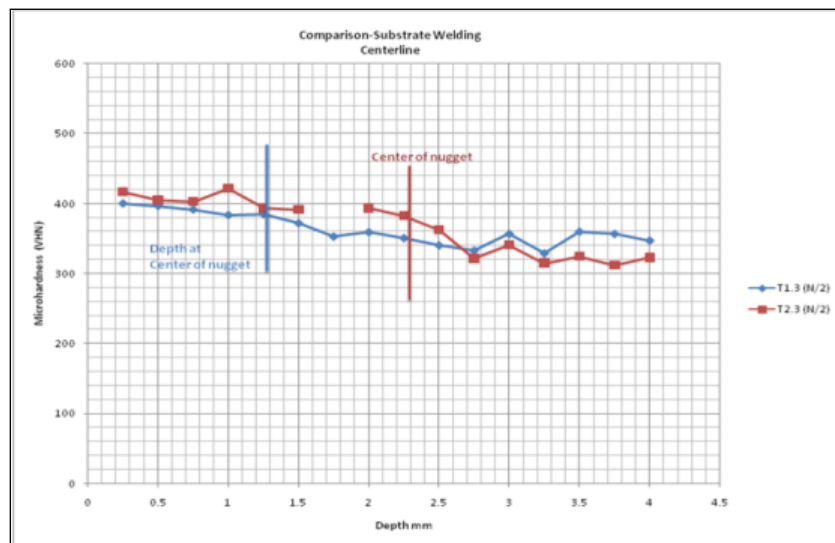


Figure 13. Microhardness data for substrate welding experiment

**Stir over deposit microhardness:** Microhardness test data for the stir over deposit (Runs: T1-103007.1 and T2-102907.1) along N/2 of the SZ revealed that the hardness had increased noticeably for the run with Tool-2 (Figure 14) but not as much for the run with Tool-1. Similar trends were observed when the microhardness data was compared at N/4 and 3N/4. As mentioned earlier this could be possible due to the more dislocation density which could have been created due to processing at lower temperatures. In both the experiments it was observed that hardness profiles in the laser deposit and substrate region beyond the nugget closely followed each other indicating that deposit hardness was uniform.

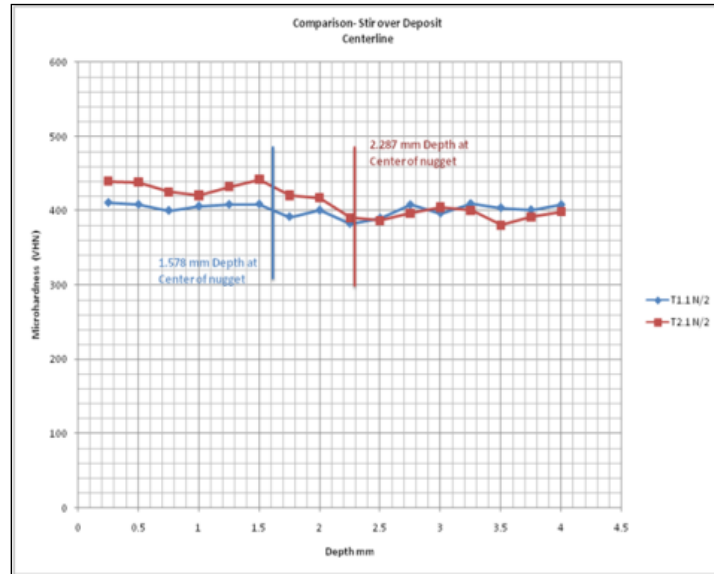


Figure 14. Microhardness data for stir over deposit experiment

**Deposit over stir microhardness:** Increased hardness was observed in the laser deposition dilution zone inside the FSP nugget (Figure 15). This was true for all the nugget regions where the laser interacted. It was also noted that the deposit was softer than the dilution zone and that is the reason for the initial surge in hardness. In case of double pass laser deposition it was observed that hardness values decrease as a function of depth before stabilizing in the stir zone which was not affected by the laser dilution zone. The HAZ of the laser interaction which was within the FSP nugget resulted in lower hardness.

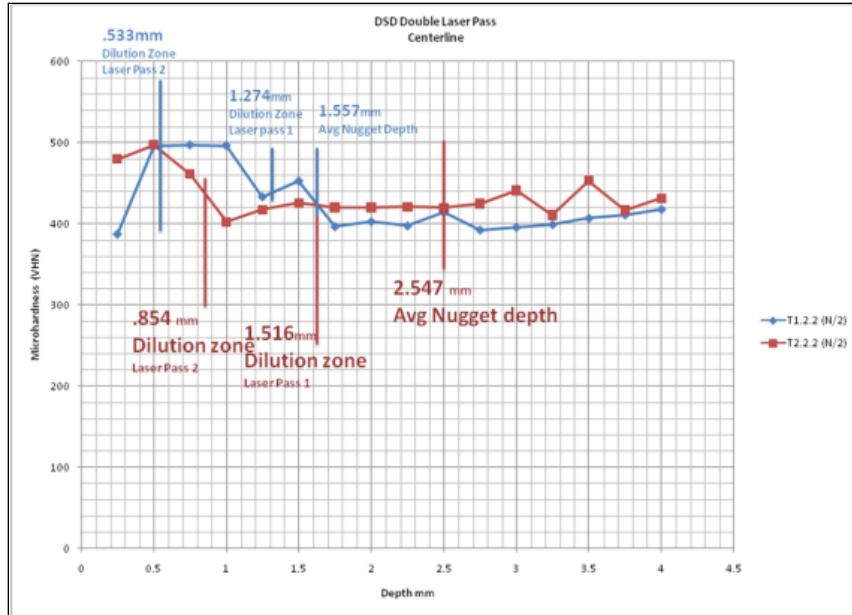


Figure 15. Microhardness data for deposit over stir experiment

**Tool Wear And Processing Defects:** Pilchak *et al.* [15] reported sub micron tungsten tool inclusions form the W-25% Re tool during FSP of investment cast, hot isostatically pressed Ti-6Al-4V. W is a beta stabilizer and being higher in the atomic number shows up bright in the SEM images (Figure 16). Densimet-176, also a W based alloy was used for this experiment and a bright stripe was observed below the processing defect formed inside the nugget region. EDS analysis performed on this area confirmed the presence of W.

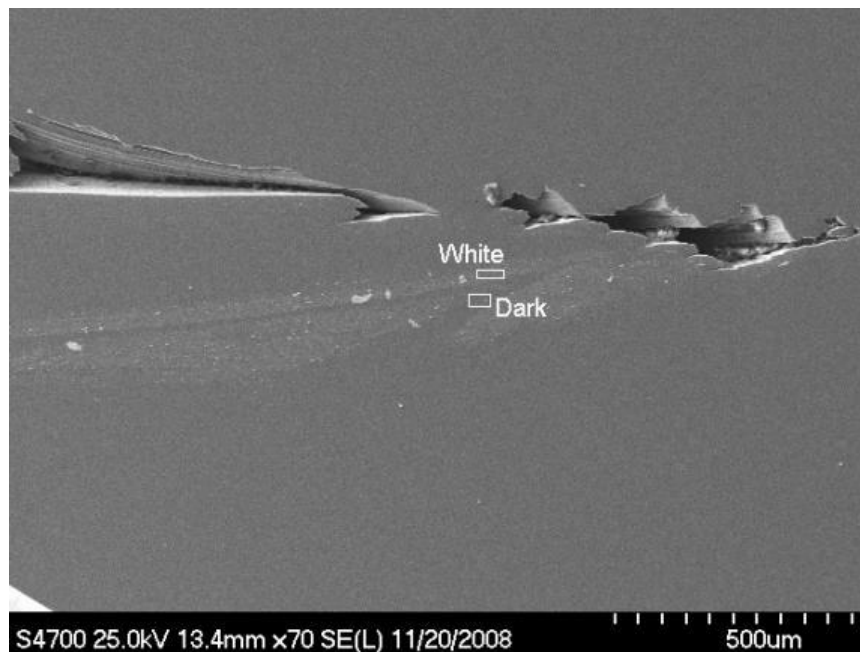


Figure 16. Processing defect observed in substrate weld experiment

This processing defect was observed ~ 1.9mm from the surface of the stir. A tool profile when superimposed on the nugget region revealed that the defect had formed in close proximity to 2<sup>nd</sup>-3<sup>rd</sup> shoulder interface. Processing voids could have been formed for a variety of reasons. One cause of this could be related to the laser deposits prepared with un-optimized deposition parameters. There were porosities in the laser deposit which was revealed when the deposit c/s was analyzed. These porosities could have accumulated on the advancing side of the tool during processing resulting in a macro void. The lead angle on the tool helps in providing a downward forge force and the absence of this lead angle due to system constraints during this FSP experiment could have also contributed to this defect.

### **Fatigue Life Estimation**

Fatigue life tests were not performed on the FSP laser deposit samples however certain predictions can be made about the fatigue life performance based on previous published work. Four point bend tests and micropillar compressive tests conducted by Pilchak et al. [16] reported increased fatigue life and compressive yield strengths in FSP cast Ti-6Al-4V. It was concluded in their study that the improved fatigue life could have been attributed to the reduced slip length from several hundred micrometers of the  $\alpha$  colony size to the primary  $\alpha$  grain size which was around 1 $\mu$ m. The equiaxed primary  $\alpha$  microstructure showed a 12% increase in the compressive yield stress. The SZ microstructure found in our study closely resembles the microstructure observed by Pilchak et al and we expect a similar fatigue response. M.Peters et al [17] have reported that reducing the  $\alpha$  grain size from 12 $\mu$ m-15 $\mu$ m to 1 $\mu$ m-2 $\mu$ m in an equiaxed Ti-6Al-4V alloy corresponded with about 25% increase in fatigue strengths at 10<sup>7</sup> cycles.

### **Conclusion**

Friction stir processing of the laser deposited Ti-6Al-4V deposits was performed and optimum processing parameters were obtained. The microstructure of the nugget regions obtained in the substrate weld, stir over deposit and deposit over stir experiments was presented. It was observed that FSP modifies the BM microstructure to a highly refined equiaxed primary  $\alpha$  grain microstructure. Large equiaxed grains were observed in the experiment where subsequent deposition was carried over the stir. A decreasing grain size was also observed in the dilution zone inside the nugget from the stir surface to the bottom of the dilution zone. Presence of a band approximately 100 $\mu$ m wide consisting of untransformed grains which did not experience  $\beta$  transus was also observed in all the samples around the dilution zone formed from laser interaction. FSP imparted hardness in the substrate weld experiment and the hardness imparted by Tool-2 was higher. It was also noted that the hardness in the dilution zone inside the nugget region was also harder than the SZ nugget. Tool wear was observed during this process, EDS analysis of the nugget showed the presence tungsten particles. Previous studies indicated that highly refined microstructure formed from FSP in Ti-6Al-4V has been able to increase the fatigue life by delaying the fatigue crack initiation. Similar performance is expected from the results obtained in this study.

### **Acknowledgments**

This research was supported by the National Science Foundation grants DMI-9871185 and IIP-0637796, the grant from the U.S. Air Force Research Laboratory contract # FA8650-04-

C-5704. The support from Boeing Phantom Works, Product Innovation and Engineering, LLC, Spartan Light Metal Products Inc, Missouri S&T Intelligent Systems Center, and Missouri S&T Manufacturing Engineering Program, is also greatly appreciated.

### References

- [1] Xinhua Wu, Jing Liang, Junfa Mei, C. Mitchell, P.S Good win, W Voice, “Microstructures of Laser Deposited Ti-6Al-4V” *Materials and Design* 25 (2004) 137-144
- [2] Yaxin Bao, Thesis, Mechanical properties and microstructure study for direct metal deposition of Titanium alloy and tool steel, 2007
- [3] H.Rubisoff, J.Querin, D.Magee, J.Schneider, “Microstructural Evolution in Friction Stir Welding of Ti-6Al-4V”, *Material Science and Technology (MS&T)* 2008
- [4] A.J.Ramirez and M.C.Juhas, “Microstructural Evolution in Ti 6Al-4V Friction Stir Welds” *THERMEC’2003, Mat.Sci.For. (426-432)* 2003, 2999-3004
- [5] A.L.Pilchak, Z.T.Li, J.J.Fisher, A.P. Reynolds, M.C.Juhas, J.C.Williams, “The relationship between Friction Stir Process (FSP) parameters and microstructure in investment cast TI-6AL-4V”, 2007. TMS Annual Meeting. pp. 419-427
- [6] Christian B. Fuller, Murray W.Mahoney, and William H.Bingel, “Surface modification with Friction Stir Processing”, 2006. *Surface Engineering-Proceedings of the 4th International surface congress.* pp. 95-101
- [7] W.M.Thomas et al., “Friction Sit Butt Welding,”: International patent Application No: PC7/GB92/02203 and G.B Patent Application No. 9125978.9, 1991. U.S Patent No. 5460317 Oct 1995
- [8] G.K. Lewis, E. Schlienger, “Practical considerations and capabilities for laser assisted direct metal deposition ,” 2000, *Materials and Design* 21 (4), pp. 417-423
- [9] ASTM E112: Standard test method for determining average grain size
- [10] A.L. Pilchak, M.C. Juhas and J.C.Williams, “A comparison of Friction Stir Processing of Mill Annealed and Investment Cast Ti-6Al-4V”: 9-10, 2008, *Welding in the world*, Vol. 52, pp. 60 -68
- [11] A.L. Pilchak, M.C. Juhas and J.C.Williams, “Microstructural Changes Due to Friction Stir Processing of Investment-Cast Ti-6Al-4V”: *Metall. Mater. Trans. A.* (2007) vol.38, pp.401-408
- [12] M.Peters, G.Lütjering, and G.Ziegler, *Z Metallkd.*,1983, vol 74, 274-282
- [13] Yu Zhang, Yutaka S Sato, Hiroyuki Kokawa, Seung Hwan C.Park, Satoahi Hirano, “Microstructural characteristics and mechanical properties ofTi-6Al-4V friction stir welds,” 2008, *Materials Science and Engineering*, Vols. A 485 (1-2), pp. 448-455
- [14] T. Seshacharyulu, S.C. Medeiros, W.G. Fraizer, Y.V.R.K.Prasad, “Microstructural mechanisms during hot working of commercial grade Ti-6Al-4V with lamellar starting structure”: *Materials Science and Engineering A325(2002)* 112-125
- [15] A.L. Pilchak, M.C. Juhas, and J.C. Williams, “Observations of Tool-Workpiece Interactions during Friction Stir Processing of Ti-6Al-4V,” *The Minerals, Metals & Materials Society and ASM International* 2007
- [16] A.L.Pilchak, D.M.Norfleet, M.C.Juhas and J.C.Williams, “Friction Stir Processing of Investment-Cast Ti 6Al-4V”, *Microstructure and Properties: Metallurgical and Materials Transactions A: Physical Metallurgy and Material Science* 39 (7), pp1519-1524

- [17] M.Peters, A. Gysler and G.Lütjering, "Influence of microstructure on the fatigue behavior of Ti-6Al-4V," Titanium '80 Science and Technology, Proceedings of the Fourth International Conference on Titanium, Kyoto, Japan,(1980) pp 1777-1786